

Decay pathways of small gold clusters^{*}

The competition between monomer and dimer evaporation

M. Vogel^{1,a}, K. Hansen², A. Herlert¹, and L. Schweikhard^{1,3}

¹ Institut für Physik, Johannes-Gutenberg-Universität Mainz, D-55099 Mainz, Germany

² Institute for Physics, University of Jyväskylä, FIN-40351 Jyväskylä, Finland

³ Institut für Physik, Ernst-Moritz-Arndt-Universität Greifswald, D-17487 Greifswald, Germany

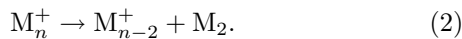
Received 2 November 2000

Abstract. The decay pathway competition between monomer and dimer evaporation of photoexcited cluster ions Au_n^+ , $n = 2-27$, has been investigated by photodissociation of size-selected gold clusters stored in a Penning trap. For $n > 6$ the two decay pathways are distinguished by their experimental signature in time-resolved measurements of the dissociation. For the smaller clusters, simple fragment spectra were used. As in the case of the other copper-group elements, even-numbered gold cluster ions decay exclusively by monomer evaporation, irrespective of their size. For small odd-size gold clusters, dimer evaporation is a competitive alternative, and the smaller the odd-sized clusters, the more likely they decay by dimer evaporation. In this respect, Au_9^+ shows an anomalous behavior, as it is less likely to evaporate dimers than its two odd-numbered neighbors, Au_7^+ and Au_{11}^+ . This nonamer anomaly is typical for copper-group cluster ions M_9^+ ($\text{M} = \text{Cu}, \text{Ag}, \text{Au}$) and a similar behavior is found in the anionic heptamers M_7^- . It is discussed in terms of the well-known electronic shell closing at $n_e = 8$ atomic valence electrons.

PACS. 36.40.Qv Stability and fragmentation of clusters – 36.40.Wa Charged clusters

1 Introduction

The fragmentation pathways of singly charged metal clusters have been studied for several monovalent elements [1–12] and are an important tool in understanding cluster energetics and dynamics. After moderate excitation above their dissociation threshold singly charged metal cluster ions show a competition between the evaporation of a single neutral atom and a neutral dimer



Pronounced odd-even-alternations in the pathway branching ratio have been found for the clusters of the elements of group 1 and 11 (or 1B) of the periodic table and have been ascribed to the clusters' electronic structure. Studies of the alkali-metal clusters Li_n^+ ($n = 4-42$) [1], Na_n^+ ($n = 5-40$) [2] and K_n^+ ($n = 5-200$) [3], and of the monovalent noble metal clusters Cu_n^+ ($n = 2-17$) [5,12], Ag_n^+ ($n = 3-21$) [4,6] and Au_n^+ ($n = 3-23$) [7] show that small odd-numbered clusters of these elements evaporate a neutral dimer while the other cluster sizes evaporate neutral monomers. A similar behavior has also been found for anionic clusters, Cu_n^- ($n = 2-8$) [10], Ag_n^- ($n = 2-11$) [9] and Au_n^- ($n = 2-15$) [8,11]. In the following, we present a

quantitative study of the relative branching coefficients as a function of cluster size for the case of small gold clusters ions Au_n^+ . The experimental results are compared with the investigations mentioned above and rationalized in terms of a liquid drop model with odd-even and shell-structure terms.

2 Experimental method

A detailed description of the experimental setup and various aspects of the use of Penning traps has already been given elsewhere [13–15]. In general, the experimental procedure consists of the following steps:

- The cluster ions are produced in a Smalley-type laser vaporization source [16,17].
- They are transferred to the Penning trap where they are captured in flight.
- The cluster size of interest is selected by resonant ejection of all other clusters and remains stored.
- A Nd:YAG pumped dye laser is used for pulsed photoexcitation at photon energies of 2-6 eV.
- The resulting cluster ion ensemble is ejected from the trap into a time-of-flight (TOF) mass spectrometer with single-ion counting after a storage period of up to 60 ms.

By variation of the storage period between photoexcitation and ejection it is possible to monitor the delayed decay process time-resolved.

^{*} Part of the doctoral thesis of M. Vogel.

^a e-mail: manuel.vogel@uni-mainz.de

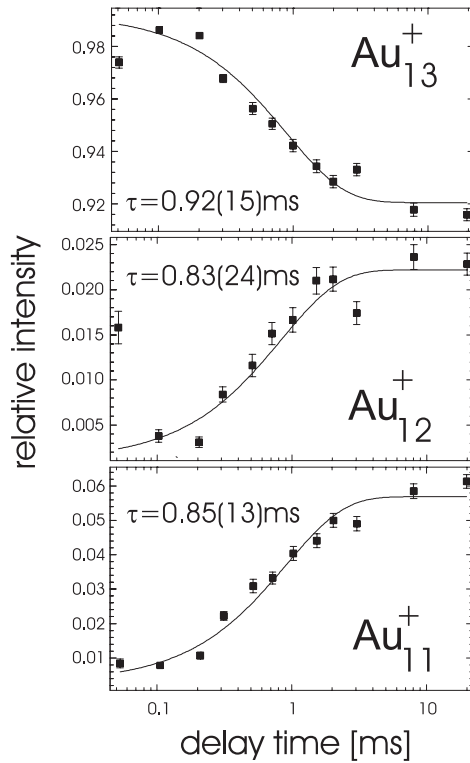


Fig. 1. Relative cluster intensities as a function of the delay period between photoexcitation and detection. Example of the decay $\text{Au}_{13}^+ \rightarrow \text{Au}_{12}^+, \text{Au}_{11}^+$ after excitation with a 10 ns laser pulse at 5.00 eV photon energy and a pulse energy of 75 μJ .

As an example, Fig. 1 shows the fragmentation of Au_{13}^+ with simultaneous evaporation of monomers and dimers. Note, that the decay constants of monomer and dimer evaporation agree within the uncertainties and both types of fragment clusters Au_{12}^+ and Au_{11}^+ are being built up with the same time constant as the one Au_{13}^+ clusters decay with. Furthermore, a sequential decay can be excluded since the abundance of Au_{12}^+ at short delay times is not sufficient to explain the increase of the Au_{11}^+ signal. This situation has already been discussed in detail for the case of Ag_{13}^+ in [6]. In the present example, about 2.5 times more dimer fragments than monomer fragments are produced, leading to a relative dimer yield of $d(13) = 0.68(5)$.

3 Results

For all cluster sizes $n > 6$ delayed photodissociation has been monitored in a time-resolved manner and $d(n)$ has been determined as described above. For $n = 2$ to 6 no delayed dissociation has been observed in the experimental time window (10 μs to 60 ms) for photon energies above 2.53 eV. However, the TOF spectra after photoexcitation (Fig. 2) show unambiguously that Au_2^+ , Au_4^+ and Au_6^+ decay by monomer evaporation, whereas Au_3^+ and Au_5^+ decay by dimer evaporation, only. Fast sequential decay can be ruled out by energetic arguments, as the excitation energy is far too small to initiate a sequential decay out-

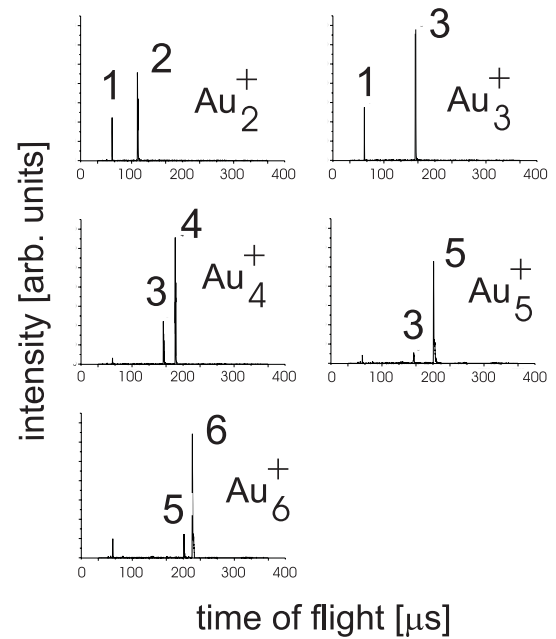


Fig. 2. Time-of-flight spectra of Au_n^+ , $n = 2-6$ after size selection and photoexcitation at 3.48 eV showing the respective decay pathways. The Au^+ signal in the spectra of Au_{4-6}^+ is due to incomplete mass selection prior to laser excitation.

side the experimental time window. Note, that for Au_3^+ monomer and dimer evaporation differ only by the location of the excess charge after the decay. Thus the phase space of the two pathways is quite similar and, provided that the decay is statistical, the branching ratio is determined by energetics. Therefore, the present observation confirms that the ionization potential of the dimer is higher than that of the monomer [18].

The relative dimer yields $d(n)$ for cluster sizes $n = 2-27$ are given in Fig. 3. While all even-numbered cluster sizes show monomer evaporation only, for the odd-numbered clusters there is a transition from predominant dimer evaporation to predominant monomer evaporation with increasing size. For the sizes $n = 7, 9, 11, 13$ and 15 both monomer and dimer evaporation is observed. The transition from monomer to dimer evaporation is monotonous with the exception of Au_9^+ which has a lower dimer yield than its two odd-numbered neighbors Au_7^+ and Au_{11}^+ .

4 Discussion and comparison with related results

For the following comparison with results for the other elements of the copper group, Fig. 4 introduces another representation of the experimental findings. A black background indicates monomer evaporation and a grey background dimer evaporation. The fragmentation pathway branching ratio is represented by the respective areas. As described above, there are three ranges: Small clusters show either monomer or dimer evaporation, depending on

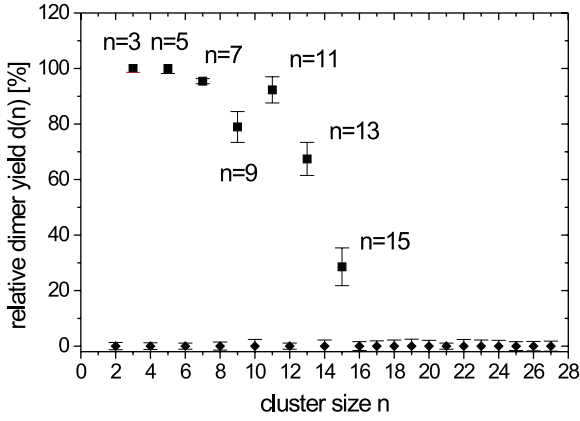


Fig. 3. Relative dimer yield as a function of cluster size. For each cluster size, the excitation energy is chosen for a decay time constant of the order of 1 ms. The error bars reflect the statistical uncertainties of the dimer and monomer fragment signals.

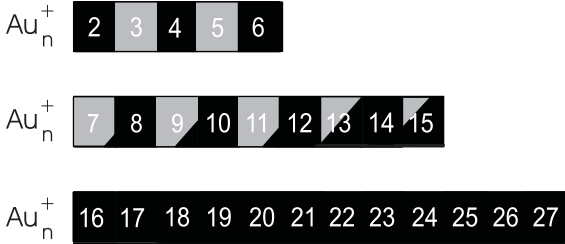


Fig. 4. Schematic representation of the decay pathways of Au_n^+ . Black: monomer evaporation, grey: dimer evaporation.

whether they are even or odd size, respectively. Large clusters decay by monomer evaporation only. In the medium range of $7 \leq n \leq 15$ the odd-size clusters show dimer evaporation in competition with monomer evaporation. For comparison, previous results on metal clusters Cu_n^+ [4,6], Ag_n^+ [12] and on Cu_n^- [10], Ag_n^- [9] and Au_n^- [11] are added in Fig. 5. The same graphic representation as in Fig. 4 is used with only the dominant decay channels indicated unless the branching is symmetric. These results have mainly been obtained by collision-induced dissociation (CID). Obviously, all noble metal clusters show a similar fragmentation behavior. The anomalous behavior of Au_9^+ is even more pronounced for Cu and Ag clusters. In order to model the size dependence of the competition between dissociation pathways we have applied the liquid drop model with an odd-even term and a correction for the electronic shell structure [19,20]. The total binding energy is given by

$$E(n) = An - Bn^{2/3} - Cn^{-1/3} - \Delta_n(-1)^n + E_{s,n} \quad (3)$$

where $A = 3.81$ eV is the average binding energy of an atom in the bulk [21], B is the surface energy prefactor of 2.95 eV given by the surface tension $\sigma = 9.27 \times 10^{18}$ eV/m² [22] and the atomic radius $r_0 = 1.59$ Å [22], C is the Coulomb-term prefactor of $e^2/(8\pi\epsilon_0 r_0) = 4.53$ eV, Δ_n

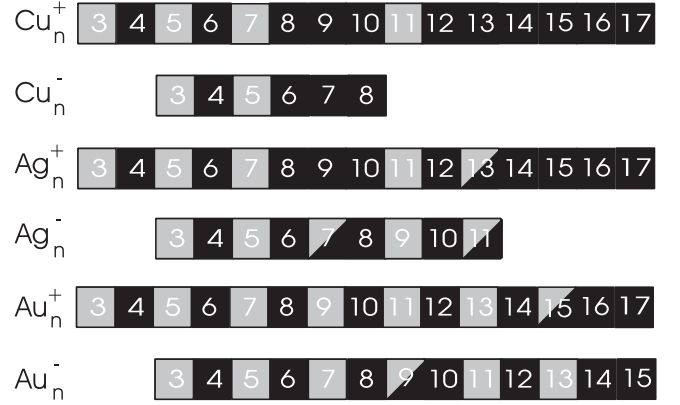


Fig. 5. Schematic representation of the dominant decay pathways of singly charged coinage metal clusters (present results and results from [4,6,9–11]). The figure is arranged so that cluster sizes in the same column have the same number of atomic valence electrons.

describes the size-dependent odd-even staggering of the dissociation energies and $E_{s,n}$ is the shell energy. Thus, the monomer and dimer dissociation energies are given by

$$\begin{aligned} D_{n,1} &= E(n) - E(n-1) \\ &\approx A - \frac{2}{3}Bn^{-1/3} + \frac{1}{3}Cn^{-4/3} - 2\Delta_n(-1)^n + D_{s,n} \quad (4) \\ D_{n,2} &= E(n) - E(n-2) - D_2 \\ &\approx 2A - \frac{4}{3}Bn^{-1/3} + \frac{2}{3}Cn^{-4/3} + D_{s,n} \\ &\quad + D_{s,n-1} - D_2 \quad (5) \end{aligned}$$

where D_2 is the binding energy of the neutral gold dimer of 2.29(2) eV [23] and D_s represents the shell correction to the liquid drop dissociation energy and is thus expected to be a sawtooth shaped function of mean zero with a slow increase towards the shell closing and a steep decline afterwards, which is the functional form used here. We have used $\Delta_n = 1.5n^{-1}$ eV and shell gaps of -0.7 eV between $n = 3$ and $n = 4$, -0.5 eV between $n = 9$ and $n = 10$ and -0.2 eV between $n = 21$ and $n = 22$. This choice of parameters represents the monomer dissociation energies [24] within 5% for $n > 6$. The size dependence of Δ is adjusted to the data and does not represent any modelling.

A measure for the dominance of the dimer branch is given by

$$P_1(n) = \frac{D_{n,1} - D_{n,2}}{D_{n,1}}. \quad (6)$$

The larger $P_1(n)$ is, the more dominant the dimer branch will be as it becomes energetically favored. Figure 6 shows the values of $P_1(n)$ as a function of the cluster size. The two horizontal lines indicate three ranges: monomer evaporation only ($P_1 \lesssim -0.17$, all even-numbered and all $n > 15$), decay pathway competition ($-0.17 \lesssim P_1 \lesssim 0.02$), and dimer evaporation only ($P_1 \gtrsim 0.02$). The observed behavior of Au_9^+ is in agreement with the values of $P_1(n)$.

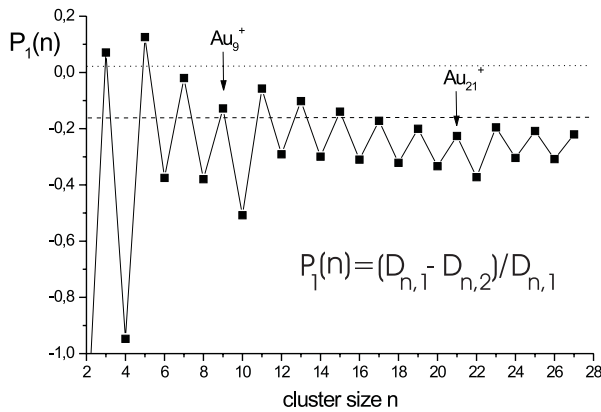


Fig. 6. $P_1(n)$ from the modified liquid drop model. For details see text.

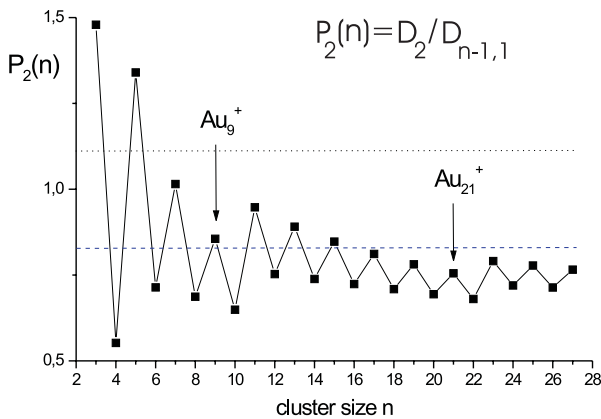


Fig. 7. $P_2(n)$. The use of the dotted and dashes lines is the same as in Fig. 6 (for details see text).

It is also instructive to compare the neutral dimer binding energy D_2 with the monomer dissociation energy $D_{n-1,1}$ of the next smaller cluster [7]. Thus, a parameter

$$P_2(n) = D_2 / D_{n-1,1} \quad (7)$$

may be defined. If one assumes that the frequency factors for monomer and dimer evaporation are identical and heat capacities are constant it is possible to show by energetic arguments that dimer evaporation is expected for $P_2(n) > 1$ while monomer evaporation is expected to dominate if $P_2(n) < 1$ [7]. By showing a pathway competition for values close to $P_2(n) = 1$ the present observations are in agreement with this simple picture (Fig. 7). Again, $P_2(n)$ agrees with the observed nonamer anomaly.

5 Conclusion

Dissociation pathway branching ratios have been determined for gold clusters Au_n^+ , $n = 2-27$. The observed non-amer anomaly is qualitatively similar to previous results on anionic and cationic coinage metal clusters. By comparison with the liquid drop model with odd-even energy and shell closure corrections it is shown that this anomaly is a consequence of the electronic shell structure. Similar effects of the influence of electronic shells on the decay pathways have been observed for polycationic metal clusters, as in the case of doubly charged alkali clusters [25] and triply charged gold clusters [26]. It will be interesting to see whether the effects also extend to the recently discovered [27] polyanionic metal clusters.

This work was funded by the Deutsche Forschungsgemeinschaft and the EU networks “EUROTRAPS” and “CLUSTER COOLING”. We further thank the Materials Science Research Center at Mainz and the Fonds der Chemischen Industrie for financial support.

References

1. C. Bréchnignac *et al.*, J. Chem. Phys. **101**, 6992 (1994).
2. C. Bréchnignac *et al.*, J. Chem. Phys. **90**, 1492 (1989).
3. C. Bréchnignac *et al.*, J. Chem. Phys. **93**, 7449 (1990).
4. S. Krückeberg *et al.*, Int. J. Mass. Spectrom. Ion Proc. **155**, 141 (1996).
5. O. Ingólfsson *et al.*, J. Chem. Phys. **112**, 4613 (2000).
6. U. Hild *et al.*, Phys. Rev. A **57**, 2786 (1998).
7. St. Becker *et al.*, Z. Phys. D **30**, 341 (1994).
8. H. Weidele *et al.*, Eur. Phys. J. D **9**, 173 (1999).
9. V.A. Spasov *et al.*, J. Chem. Phys. **110**, 5208 (1999).
10. V.A. Spasov, T.H. Lee, K.M. Ervin, J. Chem. Phys. **112**, 1713 (2000).
11. V.A. Spasov *et al.*, Chem. Phys. **262**, 75 (2000).
12. S. Krückeberg *et al.*, J. Chem. Phys. **114**, 2955 (2001).
13. L. Schweikhard *et al.*, Phys. Scripta **T59**, 236 (1995).
14. L. Schweikhard *et al.*, Eur. Phys. J. D **9**, 15 (1999).
15. St. Becker *et al.*, Rev. Sci. Instrum. **66**, 4902 (1995).
16. T. Dietz *et al.*, J. Chem. Phys. **74**, 6511 (1981).
17. H. Weidele *et al.*, Z. Phys. D **20**, 411 (1991).
18. C. Jackschath, I. Rabin, W. Schulze, Ber. Bunsenges. Phys. Chem. **96**, 1200 (1992).
19. W. Ekardt, Phys. Rev. Lett. **52**, 1925 (1984).
20. W.A. de Heer, Rev. Mod. Phys. **65**, 611 (1993).
21. N.W. Ashcroft, I. Mermin, *Solid State Physics* (Saunders College, Philadelphia, 1976).
22. *Handbook of Chemistry and Physics*, 78th edn., edited by D.H. Lide (Boca Raton, 1998).
23. M.D. Morse, Chem. Rev. **86**, 1049 (1986).
24. M. Vogel *et al.*, Phys. Rev. Lett. **87**, 013401 (2001).
25. C. Bréchnignac *et al.*, Phys. Rev. B **49**, 2825 (1994).
26. J. Ziegler *et al.*, Hyp. Int. **115**, 171 (1998).
27. A. Herlert *et al.*, Phys. Scripta **T80**, 200 (1999).